Chapter 21
Hydrogel Materials for Biomedical Application: A Review

O. Nadtoka, P. Virych, V. Krysa, V. Chumachenko, and N. Kutsevol

21.1 Introduction

Hydrogels in biomedical applications have been used for decades, and their engineering potential grows with discoveries in chemistry and biology. New approaches in diagnostic and treatment methods have led to the demand for "smart" hydrogels capable of responding to the environmental changes.

Progressive developments in this field have established promising approaches to the development of biologically significant hybrid hydrogel materials that include nano/microstructures. These materials are promising in the treatment of wounds of various genesis, drug/gene delivery, regenerative medicine, etc.

Hydrogels properties and their application are caused by their main characteristics, namely cross-linking density, mechanical strength, swelling degree, elasticity, permeability, as well as biocompatibility and sorption/sorption of drugs.

The gel is a three-dimensional polymer mesh consisting of cross-linked long chain molecules capable of absorbing large amounts of solvent, causing macroscopic changes in size. The hydrogel network can be stabilized as a giant single molecule

O. Nadtoka (✉) · P. Virych · V. Chumachenko · N. Kutsevol
Taras Shevchenko National University of Kyiv, 64, Volodymyrska Street, Kyiv 01033, Ukraine
e-mail: oksananadtoka@ukr.net

P. Virych
e-mail: sphaenodon@ukr.net

V. Chumachenko
e-mail: chumachenko_va@ukr.net

N. Kutsevol
e-mail: kutsevol@ukr.net

V. Krysa
Ivano-Frankivsk National Medical University, 2, Galytska Street, Ivano-Frankivsk 76000, Ukraine
e-mail: kwm5@ukr.net

O. Fesenko and L. Yatsenko (eds.), *Nanooptics and Photonics, Nanochemistry and Nanobiotechnology, and Their Applications*, Springer Proceedings in Physics 280, https://doi.org/10.1007/978-3-031-18104-7_21

by chemical (covalent bonds) and/or physical (ionic bonds, weaves, crystallites, complexes, hydrogen bonds, van der Waals or hydrophobic interactions) cross-links.

Special properties of hydrogels, such as high sensitivity to the physiological environment, hydrophilic nature, high content of water or biological fluids, sufficient flexibility, soft and rubbery consistency, make them similar to living tissues [1, 2].

Our works devoted to modeling the structure of chemically cross-linked hydrogels based on branched graft copolymers of dextran-polyacrylamide and studying their physicochemical properties.

Hydrogel synthesis requires the integral presence of three components: monomer, initiator, and cross-linker [3]. Solvents such as water are required to control the heat of polymerization and other properties of the hydrogels. To increase the applicability of hydrogels, it is necessary to reduce and remove by-products of reactions, in particular, unreacted monomer, initiator, and cross-linker [4]. Various hydrophilic polymers or their precursors are also used for the synthesis of hydrogels. The main classes of constituents are represented by natural polymers and their derivatives (polysaccharides and proteins), as well as synthetic polymers containing the following hydrophilic functional groups: –COOH, –OH, $–CONH_2$, $–SO_3H$, amines, and ethers [1].

Grafted copolymerization is an attractive technique for modifying the chemical and physical properties of polymers to expand their practical use. The properties of the obtained graft copolymers are controlled by the characteristics of the side chains, including molecular structure, length, and number. By covalently grafting on a polysaccharide base (chitosan, dextran, etc.), the desired functional properties of the hydrogels can be introduced.

There are three most common methods of synthesis of grafted copolymers [5–7]: grafting pre-synthesized chains to the main chain (“grafting onto” method); macromonomer synthesis (“grafting through” method), which involves the synthesis of side macrochains, and then their copolymerization with monomers, the formation of active centers along the main chain (macroinitiator synthesis) and the growth of side chains from these centers by polymerization (“grafting from” method).

Grafting can be carried out by chemical, photochemical, and γ-initiation methods. It was observed that UV initiation leads to much smaller amounts of grafts compared to other methods, while γ-radiation provides a very large number of grafts and is accompanied by the destruction of macromolecules. Grafted copolymerization is also initiated by enzymes, gamma irradiation [8], and microwave irradiation [9].

Free radical-initiated grafting is the most promising method of chemical modification, which allows the use of a wide range of synthetic polymers and natural polysaccharides and the creation of new types of hybrid hydrogels through a variety of molecular architectures.

Various redox systems are used to initiate graft copolymerization: ammonium persulfates [10], potassium [11], as well as salts of metals of variable valence, such as Fe (III), Co (III), V (V), and Ce (IV) [12–14]. The role of reducing agent is played by a polymer, such as cellulose, chitosan, and polyvinyl alcohol. Today, cerium (IV) salts are considered to be the most promising for initiating graft copolymerization,

Fig. 21.1 Schematic representation of nonionic and ionic grafted copolymers

because homopolymerization of the monomer practically does not occur during their use [15].

In our previous works [16], the intramolecular structure of dextran-polyacrylamide copolymers depending on the length of the main macrochain and the distance between the grafted chains was studied. At a constant concentration of initiator, monomer, polysaccharide, reaction time, and temperature, dextrans of different weight average molecular weights were used: 20,000, 70,000, 500,000 (denoted as D20, D70, D500), as well as dextran sodium sulfate with a weight average molecular weight of 500,000 (DSS500). It is known that macromolecules of dextrans form coils in aqueous solutions, and during polymerization on their surface-active centers, they are formed due to the presence of hydroxyl groups [17]. By "grafting from" polymerization, side chains grow from these centers. It was shown that in graft copolymers of dextran-polyacrylamide, star models are realized, and dextran sulfate–polyacrylamide spherical polymer brushes are formed [16] (Fig. 21.1).

It has been shown [16] that branched polymers form a more compact structure than linear ones. It was proved that the compactness of the macromolecular coil of star-shaped dextran-polyacrylamide copolymers is determined by the original architecture of macromolecules caused by the distance between the grafts and the length of the grafted PAA chains.

21.2 Synthesis and Characteristic of Chemically Cross-Linked Hydrogels Dextran-Polyacrylamide

To improve the hydrogels properties, the concept of creating a mesh structure based on branched polymers was used. This allows to obtain a more orderly and compact network and regulate the properties by the internal architecture of the cross-linked macromolecules.

21.2.1 Synthesis of Chemically Cross-Linked Hydrogels

Chemically cross-linked hydrogels based on grafted dextran-polyacrylamide were synthesized [18] by radical copolymerization of dextrans of different molecular weight with acrylamide (AA) using cerium (IV) ammonium nitrate (CAN) as an initiator (Fig. 21.1). Dextrans D20, D100, D500 and DS500 were used. A cross-linked polymer based on polyacrylamide was also synthesized for comparison. In the process of copolymerization, branched water-soluble copolymers of different macromolecular architecture were formed which was cross-linked by N, N-methylene-bis-acrylamide to form a 3D network. Thus, polysaccharides of different molecular weights were mesh-modeling factors. At the same time, the cross-linking density was adjusted by changing the cross-linker concentration during polymerization. The cross-linker concentration was 0.1; 0.2; 0.4; 0.6; 0.8% by weight of acrylamide to obtain hydrogels with different cross-linking densities. The obtained samples were designated as D20-PAA-x, D100-PAA-x, D500-PAA-x, and DS500-PAA-x, where x is the concentration of the cross-linker during the reaction (Fig. 21.2).

Cross-linked hydrogels based on linear polyacrylamide were obtained by a similar method without the addition of dextran. These samples were designated as PAA-x.

Copolymers based on PAA-x and D-PAA-x in anionic form were obtained by alkaline hydrolysis (Fig. 21.3).

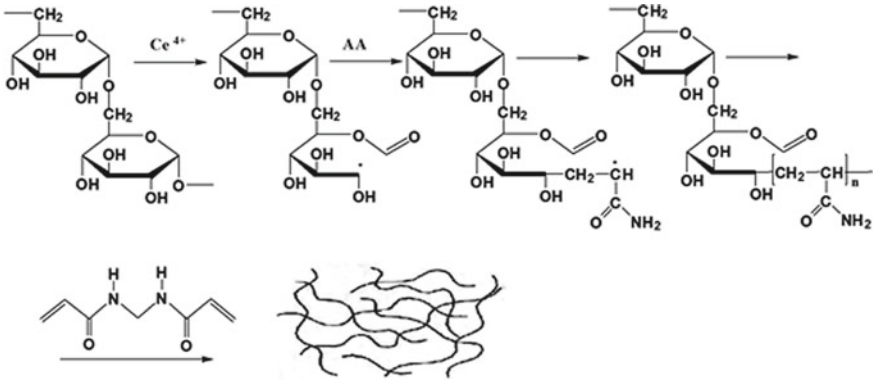

Fig. 21.2 Scheme of synthesis of chemically cross-linked hydrogels D-PAA-x

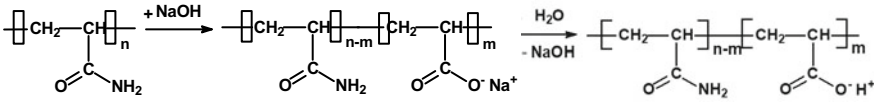

Fig. 21.3 Scheme of alkaline hydrolysis of chemically cross-linked hydrogels based on PAA-x

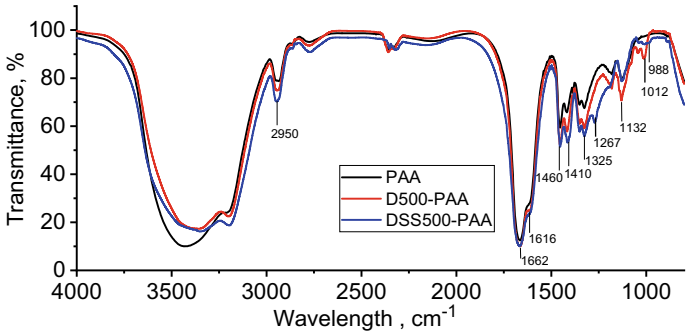

Fig. 21.4 FTIR spectra of hydrogels

21.2.2 FTIR Spectroscopy

The structure of cross-linked hydrogels in nonionic and anionic form was confirmed by FTIR spectroscopy [19].

IR spectra of PAA, D500-PAA, and DS500-PAA are shown in Fig. 21.4.

Characteristic peaks of the PAA component for all hydrogels were recorded at 1665 cm^{-1} (ν (C = O), amide I) and 1615 cm^{-1} (δ (N–H), amide II). The peak at 1450 cm^{-1} can be attributed to the valence vibrations in the functional amide groups (ν (C-N), amide III) [20].

Only the area below 1400 cm-1 is specific for dextrans [21]. The range from 1480 to 1130 cm^{-1} contains five peaks, which are at 1460, 1410, 1350, 1325 and 1132 cm^{-1}. As is known, this region contains vibrations of the deformation components in the plane of the associated and monomer alcohols and groups CH and CH_2. For aliphatic alcohols, the bands 1410 and 1350 cm^{-1} correspond to deformation vibrations in the plane of hydrogen bonds of alcohols ("association bands"). The bands at 1410 cm^{-1} correspond to both deformations of C–OH groups and deformations of CH and CH_2 groups. The strong peak at 1267 cm^{-1} has a high intensity in samples with a higher degree of hydration, such as ionized samples. In the DSS500-PAA spectrum, the presence of a sulfo group (SO_2) can be determined by the presence of absorption bands at approximately 1267 and 988 cm^{-1} belonging to ν_{as} (S = O) and ν_s (S = O) vibrations, respectively.

21.2.3 Morphological Characterization

The study of the microstructure of cross-linked hydrogels using a scanning electron microscope (SEM) shows that hydrogels based on linear and branched PAA differ in the shape of the pores. As shown in Fig. 21.5, the mesh size does not exceed 1000 nm for all hydrogels, which allows the penetration of gases, but retains microorganisms.

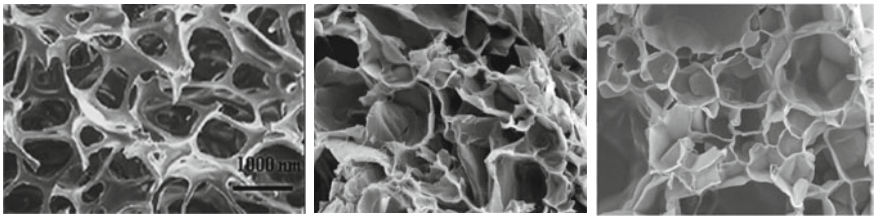

Fig. 21.5 SEM image of hydrogels based on cross-linked PAA **a**, D500-PAA **b**, and DSS500-PAA **c** (SEM Model Stereoscan 440 (LEO), Cambridge, UK)

The three-dimensional internal structure of the grafted copolymers-based hydrogels is characterized by conical pores, and this pore structure differs from the PAA-based hydrogel, which is less ordered. More enlarged pores were obtained for hydrogels based on DSS500-PAA.

For hydrogels with different cross-linking degrees, pores were obtained of differed sizes, but their characteristics were similar for a certain class of polymers. Thus, the SEM results confirm the possibility of influencing the internal structure of the hydrogel by grafting PAA onto dextran or dextran sulfate.

21.2.4 Swelling

The hydrogel as a cross-linked polymer network is able to retain water in its porous structure. Determining the amount of absorbed water is an important characteristic of the hydrogel for biomedical applications and is often described as the *swelling degree* (*S*,%) [22]. The swelling degree affects the diffusion of soluble substances passing through the hydrogel. In general, the higher the swelling degree, the greater the amount of absorbed water and the higher the rate of diffusion of the solute. Other factors, such as the microarchitecture of the polymer chain, can also play an important role. Experimentally, the swelling degree *S,%* can be determined by the following equation:

$$S_t\% = \frac{m_t - m_0}{m_o} \times 100 \tag{21.1}$$

where m_t is the mass of the hydrogel in the swollen state at time t and m_0 is the mass of the dry hydrogel.

As mentioned above, star-shaped branched copolymers of dextran-polyacrylamide (D-PAA) have advantages over linear polyacrylamide (PAA) due to the ability to regulate their internal structure during synthesis. In addition, for higher diffusion of water in the hydrogels of the PAA unit was converted into a polyelectrolyte.

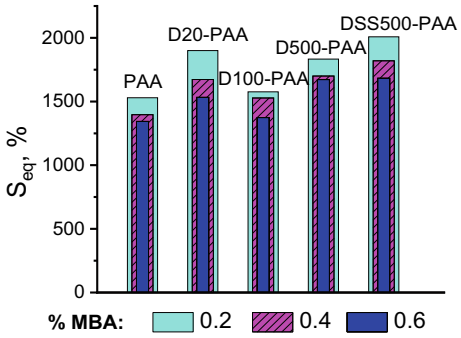

Fig. 21.6 Equilibrium swelling degree S_{eq}, % of hydrogels based on dextrans with different Mw

The behavior of hydrogels of different compositions during swelling at different cross-linking densities is shown in Fig. 21.6.

The decrease in the swelling degree of the gels decreases with increasing concentration of the cross-linker N,N'-methylene-bisacrylamide. This pattern is caused by an increase in the density of polymer chains, a decrease in pores, and an increase in the rigidity of the polymer network.

It was shown that dextrans of different molecular weights as mesh-modeling components affect the swelling ability of hydrogels in distilled water. As shown in our work [23], the internal macromolecular structure of grafted polymers depends on the size of the polysaccharide and after cross-linking leads to the formation of a more compact polymer network. In this case, the formed networks have higher porosity and a better ability to absorb water. The swelling degrees in the equilibrium state (S_{eq},%) of cross-linked polymers based on PAA, D20-PAA, D100-PAA, D500-PAA, and DS500-PAA are presented in Fig. 21.6.

In water, polyelectrolyte hydrogels dissociate and form charged macromolecules and counterions. In a three-dimensional polymer network, the charged chains are repelled from each other, and as a result, network cells begin to stretch. At the same time, the sample begins to actively absorb water and swells. Conversion of cross-linked polymers into polyelectrolytes polyacrylamide-co-polyacrylic acid (PAA-PAAc) and dextran-(polyacrylamide-co-polyacrylic acid) (D-(PAA-PAAc) significantly increases the swelling ability (Fig. 21.7). The increase in water absorption after hydrolysis is explained by the presence of carboxyl groups in polymer matrices, and their concentration is directly proportional to the hydrolysis time.

The study of swelling of cross-linked hydrogels PAA and D-PAA in salt solutions, in particular sodium chloride, is interesting because of the possibility of using hydrogels as coatings for wounds, where diffusion processes occur in the presence of dissolved low molecular weight compounds. In addition, the saturation of the hydrogel with saline (0.8% NaCl solution) makes the material close to the natural intercellular environment of living tissues and does not irritate the wound surface. The effect of ionic force on the swelling ability of the synthesized hydrogels is shown

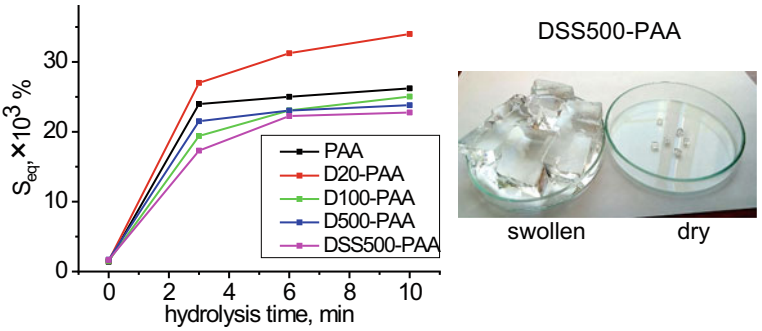

Fig. 21.7 Influence of hydrolysis time on the equilibrium swelling degree

in Fig. 21.8. It is obvious that the increase in ionic strength in the range of 0.01–1 M salt concentrations leads to a significant decrease in the swelling coefficient of hydrogels.

The high swelling sensitivity of anionic hydrogels PAA-PAAc and D-(PAA-PAAc) to ionic strength is caused by the change in charge distribution on the surface of the gel network. An increase in the concentration of Na+ ions in solution leads to a stronger "charge shielding effect" of additional cations and anion–anion electrostatic repulsion appearing [24]. Due to the reduction of the osmotic pressure difference between the polymer mesh and the external solution, the swelling of the hydrolyzed hydrogels is significantly reduced in 1 M NaCl solution.

Thus, the ability of the hydrogels to swell in the salt solution decreases compared to the swelling in distilled water. This feature is important for understanding the swelling behavior of hydrogels in physiological solutions or fluids that mimic plasma blood.

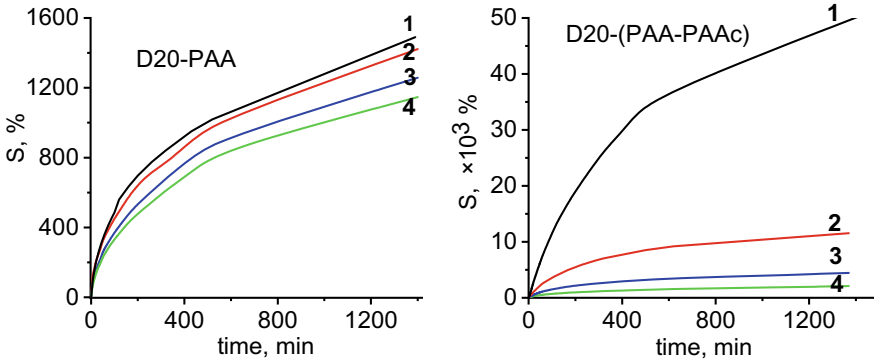

Fig. 21.8 Influence of the ionic strength of the solution on the swelling kinetics of cross-linked hydrogels (at 0.4% MBA, 10 min of hydrolysis): (1) distilled water, (2)—0.01 M, (3)—0.1 M, and (4)—1 M NaCl

21.2.5 Sorption Properties

Sorption capacity is an important characteristic of hydrogels used to remove contaminants from wounds. On the other hand, the ability to gradually release the absorbed substances can be used for the long-term delivery of drugs to the surface of the affected tissue.

The sorption capacity of hydrogels in the presence of an ionic dye is usually determined as the residual concentration of the dye in aqueous solution by spectrophotometry, where the concentration of the substance is determined by the calibration curve. The sorption degrees (Q) and sorbate release (R) are expressed by (21.2) and (21.3), respectively:

$$Q_{\text{eq}} = \frac{(C_0 - C_{\text{eq}}) \times V_1}{V_2}, \text{ mg/cm}^3 \tag{21.2}$$

$$R = \frac{(Q_{\text{abs}} - Q_{\text{des}}) \times 100}{Q_{\text{des}}}, \% \tag{21.3}$$

where C_0 and C_{eq}—initial and final concentrations of sorbate, respectively, V_1—the volume of aqueous phase (L), V_2—the volume of hydrogel without sorbate in the swollen state (cm^3), and Q_{abs} and Q_{des}—degree of absorption and desorption at equilibrium.

A pseudo-first-order kinetic model was used to determine the rate constant k of the interaction between the hydrogels and the dye in solution. The pseudo-first-order equation proposed by Lagergren [25] is often used to model fluid sorption [26]. The mathematical equation is the following

$$\frac{dQ_t}{dt} = k\left(Q_{\text{eq}} - Q_t\right) \tag{21.4}$$

where Q_{eq} and Q_t are the sorption degree ($mol\ cm^{-3}$) at equilibrium and time, t, respectively, and k is the rate constant for the equation of the pseudo-first order (min^{-1}).

As was mentioned above, branched grafted polymers have greater advantages for the sorption of charged organic molecules. Polymer networks of hybrid D-PAA form relatively structured hydrogel matrices [27] and, therefore, possess more controlled physical properties than hydrogels based on PAA. It is known that some dyes, such as diamond green ($\lambda_{\max} = 625$ nm), methylene blue ($\lambda_{\max} = 668$ nm), and basic fuchsin ($\lambda_{\max} = 540$ nm), are also used as disinfectants for the skin or for the treatment of wounds and burns [28]. Such dyes are photosensitizers and are able to produce free radical oxygen in the presence of light sources to immobilize bacterial activity [29]. These biologically active dyes loaded into the structure of highly porous hydrogels can enter the target tissues or wound surface.

Among the studied hydrogels based on branched copolymers of D-PAA, hydrogels based on ionized branched macromolecules DS500-PAA have the best sorption

properties (Table 21.1). In ionized hydrogels, the groups $-SO_3Na$ dissociate to form stationary ionized groups $-SO_3^-$. This generates electrostatic repulsion forces inside the polymer network and induces pore expansion. The formation of an ionic complex between dye molecules and ionized polymer chains promotes the absorption of a positively charged dye [30].

Studying the processes of *desorption* of methylene blue (MB) from the polymer matrix of hybrid hydrogels has shown that the release of dye occurs gradually, which provides a prolonged delivery of the biologically active substance into the environment. As can be seen from Table 21.1 and Fig. 21.9, the desorption of MB from hydrogels has significant differences in the case of non-ionized and ionized hydrogels. In hydrogels based on nonionic PAA and D500-PAA, desorption of MB is faster and caused by the presence of positively charged amide groups [31], which push out positively charged molecules MB.

Due to the presence of anionic sulfo groups, the ionized DSS500-PAA hydrogel is able to form cationic–anionic complexes with dyes, which causes a slow release of MB, as evidenced by the deeper color of the hydrogel (Fig. 21.9).

Table 21.1 Absorption–desorption characteristics of hydrogels relative to methylene blue

Sample	Absorption		Desorption		R, %
	Q_{eq}, $\times 10^{-8}$ mol cm^{-3}	k_1, min^{-1}	Q_{eq}, $\times 10^{-8}$ mol cm^{-3}	k_2, min^{-1}	
PAA-0.2	42.05	0.32	33.65	0.50	20
PAA-0.4	21.46	0.30	17.50	0.40	19
PAA-0.6	20.88	0.28	17.20	0.27	18
D500-PAA-0.2	14.79	0.27	10.07	0.36	31
D500-PAA-0.4	13.75	0.25	9.91	0.35	28
D500-ПАА-0.6	12.85	0.22	9.45	0.30	25
DSS500-PAA-0.2	127.89	0.56	126.49	0.56	1
DSS500-PAA-0.4	127.31	0.51	126.43	0.33	0.7
DSS500-PAA-0.6	127.02	0.45	126.26	0.28	0.6

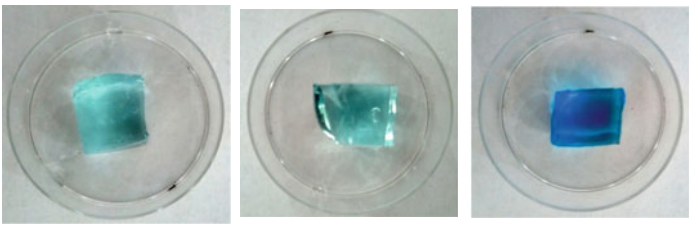

Fig. 21.9 Photo of hydrogel samples after desorption of methylene blue

As shown in our work, the sorption and desorption of diamond green and basic fuchsin occur in a similar manner, because these dyes are cationic too.

21.3 Hydrogels as Matrices for the Synthesis and Stabilization of Nanoparticles

The incorporation of metal nanoparticles (NPs) into the polymer hydrogel network is a very attractive way to develop nanocomposites for a wide range of applications.

AgNPs have many unique functions for biomedical applications due to their antibacterial properties, but high instability and low biocompatibility still remain serious clinical problems.

Hydrogels were used to protect NPs from aggregation and agglomeration. The stabilization of nanoparticles in cross-linked hydrophilic polymers is an expected effect in the production of hydrogel/AgNPs composites. As the free space inside the gel mesh can be used as a nanocontainer for the formation and growth of metal nanoparticles, the porous structures of hydrogels are suitable for the formation of AgNP in situ [32].

The modern method of obtaining silver nanoparticles by irradiation with ultraviolet light is based on the ability of D-PAA to generate free radicals in the presence of UV irradiation and act as a reducing agent against Ag^+. Hydrogel composites with AgNPs were obtained at different doses of UV irradiation (Fig. 21.10). With increasing irradiation time, the color of the samples becomes deeper, which indicates an increase in the concentration of nanoparticles.

As the SEM results show, the main advantage of UV technology is providing of controlled and uniform distribution of nanoparticles inside the hydrogel network without the addition of any other stabilizer (Fig. 21.11).

Analysis of the absorption spectra of composites based on linear and branched polymers PAA/AgNPs and D20-PAA/AgNPs with different cross-linking degrees (Fig. 21.12) shows that all nanocomposites registered a wide peak in the range of 380–850 nm. The presence of this SPR band indicates the presence of AgNPs with a wide particle size distribution.

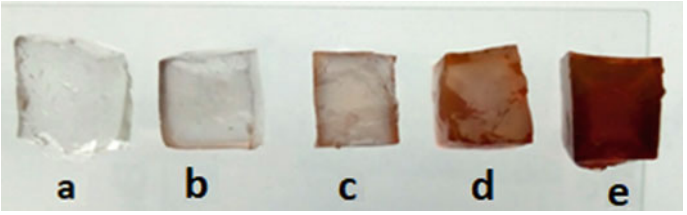

Fig. 21.10 Photo of D-PAA/AgNPs samples at different radiation doses: **a** 0 min, **b** 1 min, **c** 3 min, **d** 5 min, and **e** 10 min

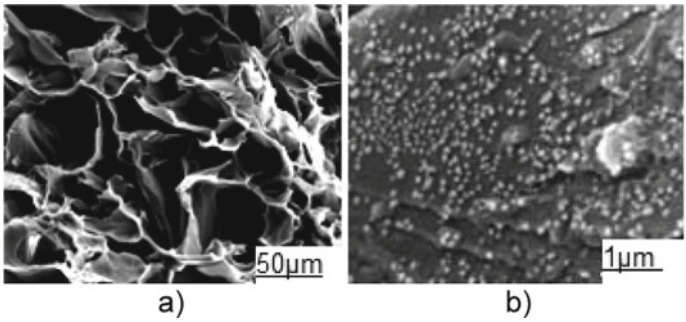

Fig. 21.11 SEM photo of hydrogel composites D20-PAA/AgNPs, obtained by photochemical method: **a** magnification of 7000 times and **b** magnification of 35 000 times

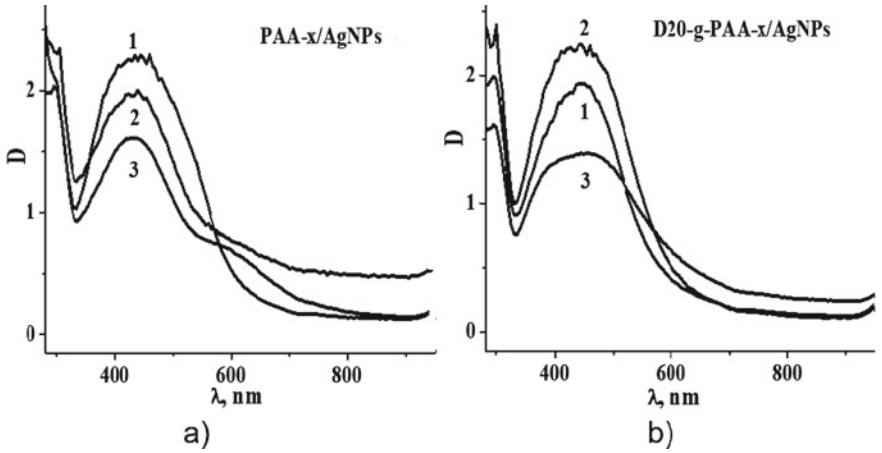

Fig. 21.12 Absorption spectra of composites PAA/AgNPs **a** and D20-PAA/AgNPs **b** at different cross-linking degrees of hydrogels: % MBA = 0.2 (1); 0.4 (2); 0.6 (3). Irradiation time 5 min

It is known that the absorption peak at 298 nm can be registered for $AgNO_3$ solution and corresponds to Ag^+ ions [33]. The procedure for obtaining a hydrogel/AgNPs composite assumes the presence of residual Ag^+ ions in the swollen cross-linked polymer, and the presence of this peak in the absorption spectrum is obvious (Fig. 21.12). All absorption bands have a complex line shape and contain various components that contribute to the overall spectrum. Three regions are well distinguished: about 380, 420, and 535 nm. These bands indicate the formation of polydisperse AgNPs of 20, 50, and 100 nm, respectively [34].

21.4 Hydrogels as Materials for Wound Dressings

Initially, polymer dressings were considered passive materials that play a minimal role in the wound healing process. In the 1960s, the first generation of polymer dressings was introduced, [35] which provided the optimal environment for wound healing. Since then, polymer hydrogels as biomaterials have attracted much attention and interest from scientists for many years.

Wound healing takes place in four stages: homeostasis, inflammation, granulation tissue formation, and reconstruction. Self-healing of the skin is usually accompanied by the formation of scars. Therefore, traditional treatment leads to the loss of the dermis and is therefore unsatisfactory, while the use of polymeric materials to create wound dressings of the new generation provides complete recovery or healing of skin tissues. It has been shown that wound healing with wet dressings is faster than with dry ones! Thus, moisturized or moisturizing dressings should be considered in skin repair and wound healing.

It has been shown that hydrogels as dressings provide all the requirements for wound healing and burns due to the following justifications [36]:

- hydrogels as porous materials are able to absorb and retain water, controlling fluid loss from the body and maintaining wetting and moisture in the wound area;
- small size of hydrogel pores protects the wound from infection and prevents the penetration of microorganisms and bacteria into the wound;
- the elastic property of swollen or hydrated hydrogels provides flexibility and elasticity to adapt to the wound surface and minimizes irritation or damage of surrounding tissues;
- hydrogel can absorb wound exudates, which promotes the processes of fibroblast proliferation and keratinocyte migration, which are necessary for complete epithelialization and wound healing;
- both compositionally and mechanically hydrogels are similar to the natural extracellular matrix; thus, they can serve as an auxiliary material for cells during tissue regeneration and a carrier in the delivery of a therapeutic agent;
- the low interfacial voltage between the surface of the hydrogel and body fluid minimizes protein adsorption and cell adhesion, which reduces the likelihood of a negative immune response;
- the mucoadhesive and bioadhesive properties of many polymers used in hydrogel materials (e.g., polyacrylic acid, polyethylene glycol, and polyvinyl alcohol) increase the time of stay of the drug on the skin/plasma membrane, leading to increased tissue permeability.

Thus, the trend toward research and development of hydrogels as polymeric dressings becomes a commercial goal.

Hybrid hydrogels based on cross-linked branched graft copolymers were converted into composites with biologically active substances that are able to show a bactericidal effect directly or under the action of light.

21.4.1 Antibacterial Wound Dressings with Silver Nanoparticles

The discovery and use of antibiotics have reduced mortality from bacterial wound infections. At the same time, antibiotic-resistant strains of microorganisms have emerged [37], prompting the search for alternative antibacterial agents. One of them was combined hydrogels [38] with silver nanoparticles. It is the structural organization of the hydrogel that determines the size of nanoparticles and effectively stabilizes them [39, 40]. Silver nanoparticles show high bactericidal activity, although the reduced form of Ag^0 silver itself does not show biological activity. In the presence of oxygen and protons in the environment, the following reactions occur:

$$4Ag + O_2 = 2Ag_2O$$
$$2Ag_2O + 4H^+ = 4Ag^+ + 2H_2O$$

It is the released Ag^+ that cause cytotoxic effects [41]. The mechanism of action of Ag^+ is based on interactions with free hydrogen sulfide groups of proteins of bacterial membranes, which leads to disruption of their function and neutralization of the transmembrane ion gradient and cell necrosis. It is important that resistance to Ag^+ develops slowly compared to antibiotics [42].

Three-dimensional polymer hydrogels loaded with AgNPs are considered to be materials with very high potential for medical therapeutic and diagnostic applications [43]. Loading of the hydrogel structure with silver nanoparticles allows to give the material antibacterial properties, and the high water content and no toxic effects on the surrounding tissues contribute to faster wound healing. Polyacrylamide is a particularly promising polymer because it is similar in peptide structure and promotes skin regeneration. PAA-based hydrogels with bactericidal properties prevent bacterial contamination of damaged tissues and reduce the risk of inflammation and ulcers.

Antibacterial properties were investigated for PAA/AgNPs and D20-g-PAA-x/AgNPs at a cross-linker concentration of 0.2, 0.4, or 0.6% by weight of the monomer.

To test the material for its ability to inhibit the growth of bacterial cultures, wild strains of gram-positive and gram-negative cultures of *Escherichia coli* and *Staphylococcus aureus*, electively obtained on Endo media and yolk-salt agar, were used. The susceptibility of strains of microorganisms was evaluated by the disk-diffusion method (Fig. 21.13).

Due to the widespread use of antibiotic-resistant strains of microorganisms, general antibiotics Cefazolin and Ceftriaxone were used as controls. Measurement of the zone of growth retardation was performed after 24 h.

According to the photos in Fig. 21.13, it was found that the used wild strains of microorganisms *E. coli* and *S. aureus* show resistance to Cefazolin and Ceftriaxone, because after some time the emergence of new colonies of these bacteria in the area of antibiotic action was rerecorded. It is known that this is a global health problem that leads to limited treatment options using antibiotics.

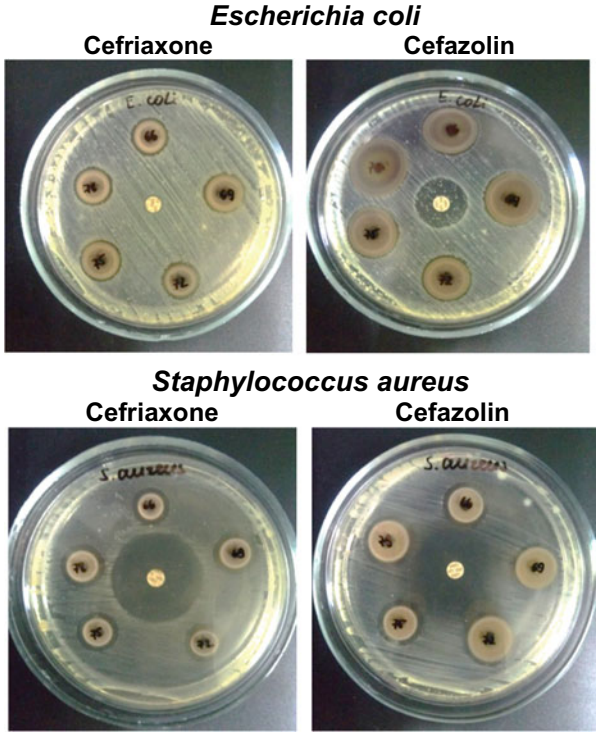

Fig. 21.13 Disk-diffusion tests of antibacterial efficacy of hydrogel/AgNPs nanocomposites against *Escherichia coli* and *Staphylococcus aureus* compared to antibiotics Ceftriaxone and Cefazolin (placed in the center)

Almost equally high sensitivity of *E. coli* and *S. aureus* strains to both antibiotic and hydrogel composites with silver nanoparticles was revealed. Although the antibacterial activity of composites is slightly lower than that of antibiotics, this study is evidence that silver nanoparticles as antibacterial agents are competitive substitutes for antibiotics and have valuable advantages because they do not cause bacterial resistance. Hydrogel composites based on branched polymers, in particular D20-PAA and D100-PAA, show advantages in bactericidal action on strains of both cultures in comparison with linear PAA.

To confirm the relationship between the density of the polymer network and the biological activity of nanoparticles obtained in this network, the sensitivity of *E. coli* to the nanocomposites of different cross-linking densities was studied (Fig. 21.14). As seen from Fig. 21.14, the photo of the disk-diffusion test demonstrates the presence of bacterial resistance to the antibiotic as the appearance of colonies in the area of its initial action. In the presence of hydrogel composites, bacterial resistance is not observed. Figure 21.14b shows an increase in the efficiency of the composite with increasing density of the polymer matrix in which the silver nanoparticles

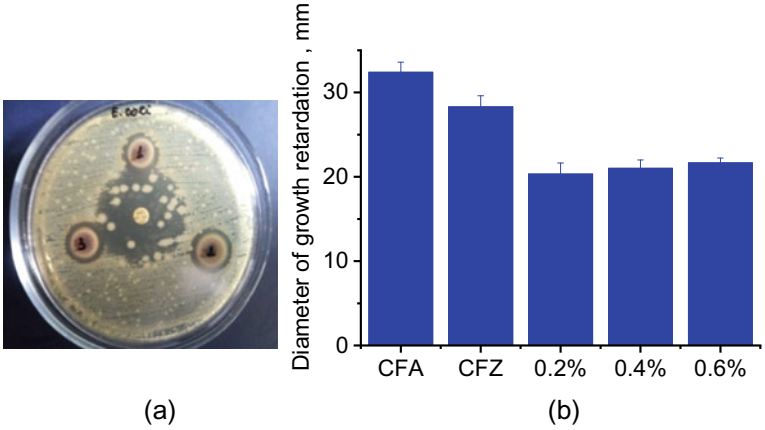

Fig. 21.14 **a** Disk-diffusion tests of antibacterial efficacy against *Escherichia coli* of hydrogel/AgNPs nanocomposites compared to the antibiotic Cefazolin (inside); **b** the dependence of the diameter of the growth retardation of *Escherichia coli* on the concentration of the cross-linker for composites D20-PAA/AgNPs

were obtained. As mentioned above, the higher the mesh density, the smaller the nanoparticles formed and the greater their bactericidal properties.

21.4.2 Comparison of Antibacterial Efficacy of Composites Hydrogel/AgNPs and Hydrogels/Chlorohexidine

To the comparison of bactericidal activity of composites hydrogel/AgNPs and hydrogels/chlorohexidine (CH), wild strain *Staphylococcus aureus* was used (Fig. 21.15).

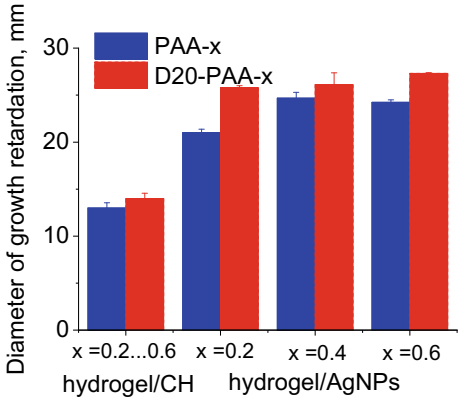

Fig. 21.15 Diameter of the growth retardation of *Staphylococcus aureus* for hydrogel composites with CH and AgNPs

As shown in Fig. 21.15, hydrogels containing silver nanoparticles inhibit the growth of *S. aureus* colonies more actively: The diameters of growth retardation for hydrogel/AgNPs are larger than that for the samples hydrogel/CH and reach 21–27 mm. It should be noted that for both hydrogel composites a larger diameter of growth retardation was obtained when using hydrogels based on branched polymers D20-PAA-x compared to analogs based on linear PAA-x. There was also a tendency to increase the activity of composites with AgNPs with increasing degree of cross-linking. Obviously, this is caused by the smaller size of the formed nanoparticles, as presented above, in which they have greater biological activity.

21.4.3 Testing of Hydrogel Composites with AgNPs on Open Wounds

The obtained hydrogel composites proved to be effective in the treatment of wounds. The therapeutic efficacy of hydrogel materials was investigated in vivo on open wounds with artificial bacterial contamination [44].

White outbred rats were used in the studies. All animal manipulations were performed in accordance with the International Convention on the Treatment of Animals.

Sterile gauze bandages were used as controls. The bandages were on the animals for 48 h. The examination was performed 3 and 5 days after surgery. At the first examination (after 72 h), bacterial culture was performed from the wound on selective Endo media and yolk-salt agar for the presence of appropriate bacterial strains.

Figure 21.16 shows the stages of wound formation and treatment over five days. For comparison, a traditional gauze material (1) was used, as well as a hydrogel sample (2) and a composite hydrogel/AgNPs (3).

The study showed significant advantages in the effectiveness of treatment with the use of hydrogels, namely no colonies of pathogenic bacteria were detected during treatment with hydrogel coatings, while when using a gauze bandage, about 200 colonies of *S. aureus* were recorded. Three days after hydrogel dressing, the wound surface was reduced by approximately 30% without any inflammation or discharge, and five days of treatment showed significant benefits of using hydrogel composites with silver nanoparticles.

The achieved efficiency of composites caused by two main factors: the humid environment of treatment, which is provided by hydrogels, and bactericidal properties due to the presence of silver nanoparticles [45].

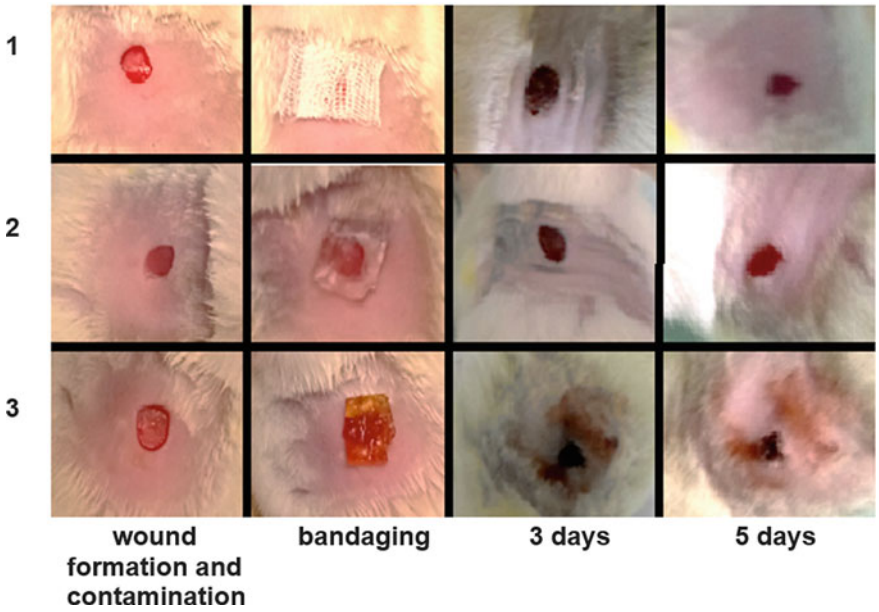

Fig. 21.16 In vivo study of the effectiveness of hydrogel dressings in the treatment of open wounds with artificial bacterial contamination: (1) traditional gauze material, (2) hydrogel sample, and (3) composite hydrogel/AgNPs

21.4.4 Testing of Hydrogel Composites with AgNPs on Open Human Wounds

Hydrogel composites with silver nanoparticles were tested as dressings for the treatment of wounds, in particular, chronic active ulcers (Fig. 21.17).

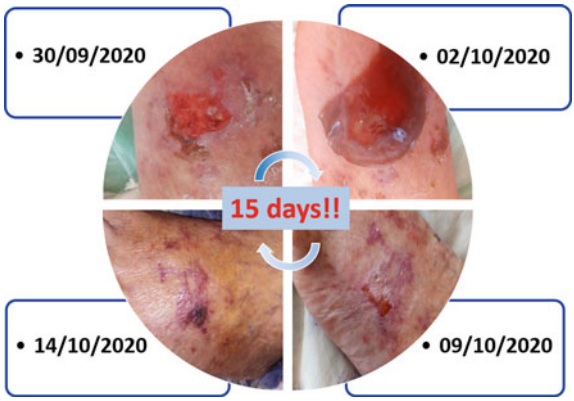

Fig. 21.17 Efficacy of hydrogel wound dressings with AgNPs in the treatment of trophic human wounds

In the previous long-term treatment (more than 2 years) of ulcers by traditional methods using analgesics, anti-inflammatory, and antibacterial drugs, patients complained of an increase in the wound surface of the ulcer, which was accompanied by pain. In a short time, when using the application of hydrogel composites with AgNPs on the same trophic ulcers, doctors proved the high effectiveness of wound healing. Positive signs during treatment were the rapid disappearance of pain, reduction in a short time the size of ulcers, and complete epithelialization of the wound within 14 days.

21.4.5 Hydrogel Materials for Photodynamic Therapy of Open Wounds

In clinical practice, aseptic dressings are used to treat wound processes. It closes the wound surface from infection and at the same time maintains a moist environment on the wound surface, which promotes tissue regeneration. Such conditions also contribute to the reproduction of pathogenic microflora, which is present on the skin. Reproduction of microflora in the wound causes the appearance of pathological processes that interfere with its healing. To prevent such consequences, solutions of antibiotics or antiseptics are used. They have bactericidal or bacteriostatic properties and provide the desired therapeutic effect. However, the rapid development of resistance of microorganisms reduces the effectiveness of antibiotics. Alternatives are agents based on inorganic compounds: ions, metal oxides and their nanoparticles, chelates, etc. They provide non-selective action and, in contrast to the effect of antibiotics on gram-positive and gram-negative microorganisms, have multiple mechanisms of action [38].

One of the promising areas of treatment of wounds and chronic ulcers is photodynamic therapy. Visible light has significant antibacterial properties, although the efficiency is inferior to ultraviolet. Unlike high-energy UV irradiation, visible light is less harmful [46]. When irradiated, it has less risk to body tissues. Bacterial photosensitizers (PS) are important additional enhancers of bactericidal efficiency of visible light. It was found that the interaction of PS with red light (405–470 nm) destroys microorganisms or creates preconditions that disrupt the metabolism of microorganisms [47, 48].

Synthetic photosensitizers are used to increase the bactericidal activity of light irradiation of certain wavelengths. By absorbing light, they are able to generate active radicals or interact with cellular targets, inactivating them. Such substances include dyes that have absorption maxima in the red and green regions of the visible range of electromagnetic oscillations. Among such compounds, the most well-known is methylene blue.

The method of photodynamic therapy (PDT) is based on the interaction of visible light and photosensitizer (PS), which during photoactivation generates short-lived cytotoxic species of radicals. Depending on the formed active particles, PDT is

classified into two types. Type I is the interaction between the excited triplet state of the photosensitizer (3PS*) and the target tissue substrates. As a result of the reaction between the photosensitizer and the substrates, new radicals are formed. They interact with molecular oxygen and other molecules in the environment. According to type II, the interaction of 3PS* and molecular oxygen leads to the formation of singlet highly reactive oxygen [$^1O_2$]. These formed free radicals and singlet oxygen interact with various cellular targets, including membranes, nucleic acids, and enzymatic complexes, disrupting their functioning [49]. Thus, the main components of PDT are as follows: (1) photosensitizer, (2) light source, and (3) molecular oxygen.

Hydrogels based on branched copolymers of D-PAA, loaded with light-sensitive photosensitizer MB (Fig. 21.9), were studied as materials for photodynamic therapy for inactivation of microorganisms under the red light [50].

The LIKA-Led device (Photonics Plus, Cherkasy, Ukraine) with laser emitters of 660 nm was used to generate light. Irradiation with a power of 100 mW for 20, 30, and 40 min leads to an irradiation dose of 21, 31.5 and 42.1 J/cm^3, respectively.

First of all, the antimicrobial activity of D500-PAA/MB (5×10^{-4}%) in suspension of *S. aureus* (10^5 CFU/ml) was studied. Hydrogel samples were placed in a bacteria suspension at mass ratio of hydrogel: suspension = 1:4. After 120 min, the equilibrium concentration of MB in solution was $10^{-4} \pm 2 \times 10^{-5}$%. The bactericidal effect caused by light irradiation (660 nm, 100 mW) was evaluated as the percentage of deaths from CFU relative to the control sample.

The study of the antibacterial efficacy of red light (660 nm) against *S. aureus* in bacterial suspension indicates the absence of its bactericidal action (Fig. 21.18). It can be explained by the low energy of light quanta and the absence of photosensitizer targets in bacterial cells. Unlike ultraviolet or blue light (380 nm and 490 nm), red light (660 nm) is less aggressive to living tissues and therefore desirable for wound healing. In this case, infrared radiation penetrates deeper into body tissues and causes heating of the entire skin and subcutaneous tissue. The therapeutic effect of infrared radiation is determined by the mechanism of its physiological action, which is to accelerate the reversal of inflammatory processes and increase tissue regeneration, local resistance, and anti-infective protection.

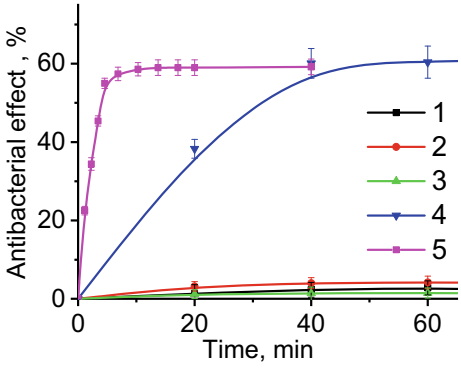

Fig. 21.18 Antibacterial effect of red light (660 nm) (1); MB (10^{-4}%) (2); pure D500-PAA (3); D500-PAA, saturated MB (5×10^{-4}%) and activated by red light (660 nm) (4); MB (10^{-4}%) activated by red light (660 nm) (5) in a suspension of wild strains of *S. aureus*. M ± SD

As shown in Fig. 21.18, methylene blue at a concentration of 10^{-4}% has no antibacterial properties in the suspension of *S. aureus*. The combination of red light and MB at 10^{-4}% resulted in a 20% reduction in CFU at a low irradiation dose of about 2 J/cm^3. Increasing the radiation dose to 6 J/cm^3 leads to inactivation of 60% CFU. A further increase in the radiation dose does not lead to an increase in bactericidal activity, which may be associated with the adaptation of the culture of *S. aureus* to the created conditions or lack of oxygen and/or dye in solution.

The study of the diffusion of MB from the hydrogel into the solution showed the gradual release of the dye in a short time. This allows for a long time to provide the required concentration of active substance in a suspension of pathogenic bacteria. Taking into account the obtained results, the antibacterial effect of hydrogel materials saturated with MB in combination with visible light was investigated. D500-PAA of the lowest cross-linking density (at 0.2% MBA), and the highest release ability was selected as the MB container. It was shown that certain components, such as pure hydrogel, light irradiation at 6 J/cm^3, and MB sensitizer, do not have antibacterial activity in the bacterial suspension (Fig. 21.19). The complex action of the hydrogel composite D500-PAA/MB and light irradiation resulted in the loss of 60% of the initial amount of CFU when incubating the hydrogel in suspension for 40 min.

In addition, it should be noted that the time to achieve the maximum bactericidal effect of MB in suspension is shorter than MB contained in the hydrogel and gradually released from it. This indicates that the hydrogels saturated with MB provide a prolonged bactericidal effect.

The disk-diffusion method was used to study the antibacterial activity of hydrogels *on a solid medium*. The antimicrobial activity of MB-saturated hydrogels was evaluated by analyzing the diameter of bacterial growth retardation [51].

D500-PAA was used as a hydrogel matrix at MB concentration of 10^{-3} and 10^{-4}%. As can be seen from Fig. 21.19, at MB concentration of 10^{-4}%, irradiation of the hydrogel with different energy doses does not lead to appreciable bactericidal activity.

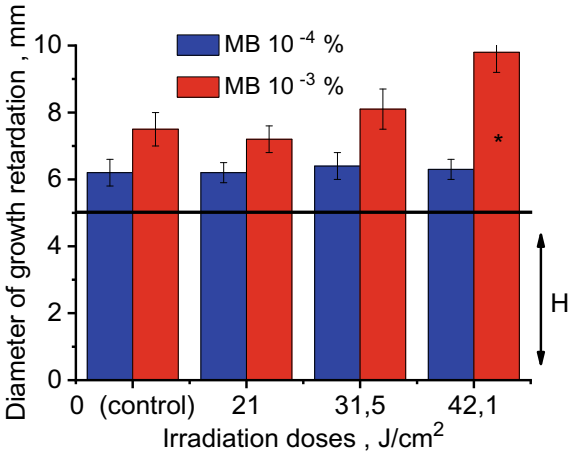

Fig. 21.19 Bactericidal effect of D500-PAA/MB, activated by red light (660 nm) on Mueller–Hinton agar against *S. aureus*. H is the diameter of the hydrogel sample, M ± SD, * $p < 0,05$

When the concentration of MB in the hydrogel increases to 10^{-3}%, the dependence of the bactericidal activity of the composites on the irradiation doses was observed and the bactericidal effect reaches about 10 mm in the diameter shown as the bacterial growth retardation around the sample.

Thus, hydrogels based on branched copolymers dextran-graft-polyacrylamide as nanocontainers for biologically active substances, in particular photosensitizers, have shown high efficacy for photodynamic antibacterial therapy and can be used in the treatment of wounds. The application of these materials saturated with photosensitizers significantly increases their effectiveness due to long-term maintenance of the required therapeutic concentrations of the substance at the site of injury. Hydrogels with high water content, low toxicity, and high biocompatibility are used to prevent or treat bacterial contamination of wounds. Their structure allows them to keep the required amount of drug substance and release it into the environment at a certain rate.

21.4.6 Hydrogel Materials for Drug Delivery

Among many antibacterial agents, antibiotics are one of the most effective and widely used drugs. However, their widespread and often thoughtless use has provoked the emergence and spread of resistant strains of bacteria. This has led to the problem of antibiotic resistance, which has become a global challenge today.

There are two main ways to overcome antibiotic resistance: the synthesis of new antibiotics and the development of new methods of antibiotic use. Hydrogels of various chemical nature can be used as promising carriers of antibiotics in biotechnology and medicine. Over the last few decades, various antibiotic-loaded hydrogels were developed as antibacterial coatings and dressings for the treatment of superficial traumatic, burn, or diabetic wounds [50, 52]. These materials release antibiotics at the wound site, thus preventing infection and promoting healing [53]. Local wound treatment with antibiotics significantly reduces the unwanted side effects that are often observed with systemic use.

This method of treating wound surfaces requires the creation of hydrogels that contain high concentrations of antibiotics. This is especially important for the care of infected wounds and burns. Antibiotic-loaded hydrogels are tested for both antibiotic-sensitive and antibiotic-resistant bacteria [54].

Because successful anti-inflammatory treatment of wounds is directly dependent on the continuous action of antimicrobials, hydrogels loaded with antibiotics must release the active substance for a long time (prolonged). Controlled and sustained release of the antibiotic in the affected area is an important requirement to prevent the formation of biofilms [53]. In addition, the continuous delivery of the drug to the application site provides a significant increase in the time intervals required to change the dressing on the wound. As noted, the nature of the polymer and the degree of cross-linking are the main factors that regulate the ability of hydrogels to deliver drugs and release them at the target site.

Table 21.2 Content of Cefuroxime in the synthesized hydrogels (g of antibiotic per g of dried hydrogel) and its release into the water

Sample	Content, g/g	Time of contact with water, h		
		0.5	1	6
PAA-0.4-Cef	1.64	28	42	55
D20-PAA-0.4-Cef	3.52	24	30	42
D100-PAA-0.4-Cef	3.40	22	27	38
D500-PAA-0.4-Cef	3.34	19	34	40
DSS500-PAA-0.4-Cef	3.31	27	37	51

Chemically cross-linked hydrogels based on branched copolymers D-PAA were used to create antimicrobial coatings for the treatment of infected wounds. These hydrogels were loaded with the required concentration of antibiotics, and their local drug release was intended to overcome the side effects of systemic overdose. Antibiotic samples were tested in vitro for pathogenic bacteria and in vivo as antimicrobial dressings.

To prepare antibiotic hydrogel samples, dried hydrogel samples were placed in an aqueous solution of Cefuroxime (Cef) (166.6 mg/ml) and incubated at 25 °C for 18 h. The amount of loaded antibiotic in the hydrogel sample was evaluated by subtracting the amount of Cefuroxime remaining in solution from the initial content. All concentrations were determined by high-performance liquid chromatography with ultraviolet detection (HPLC–UV). Swollen hydrogels in this solution were used for further studies of their ability to release the antibiotic. Determination of the concentration of antibiotic released into the solution was performed by HPLC–UV at regular intervals.

As given in Table 21.2, the content of Cefuroxime is the highest for hydrogels that were synthesized using dextran as a structuring component.

Contact of the antibiotic-loaded hydrogels with water leads to desorption of drug molecules into solution. For all samples, the initial release is characterized by a low rate within 3 h. As given in Table 21.2, the sample PAA-0.4-Cef has the highest release rate. The content of Cefuroxime in this hydrogel decreased by 55% after 6 h of contact with water. In contrast, D-PAA-0.4-Cef, being initially more loaded with Cefuroxime, releases the drug into solution more slowly than PAA-0.4-Cef.

Thus, D/DSS-PAA-0.4-Cef hydrogels have some advantages over other studied hydrogels. They are able to provide a prolonged antibacterial effect on the wound surface. It is assumed that they are promising biomaterials for local application as antimicrobial dressings.

Antibacterial activity in vitro was studied by the above-described disk-diffusion method. All synthesized hydrogels loaded with Cefuroxime showed high activity against bacterial strains of *S. aureus*, *E. coli,* and *Klebsiella spp.* (Table 21.3).

The antimicrobial activity of hydrogels depends on the concentration, but even at low doses, antibiotic-loaded hydrogels show high efficacy against harmful microorganisms (Fig. 21.20).

Table 21.3 Antimicrobial activity of Cefuroxime-loaded hydrogels

Sample	Diameter of bacterial growth retardation, mm		
	S. aureus	*E. coli*	*Klebsiella spp.*
PAA-0.4-Cef	27	23	20
D20-PAA-0.4-Cef	26	21	20
D100-PAA-0.4-Cef	30	22	20
D500-PAA-0.4-Cef	25	22	23
DSS500-PAA-0.4-Cef	29	21	22

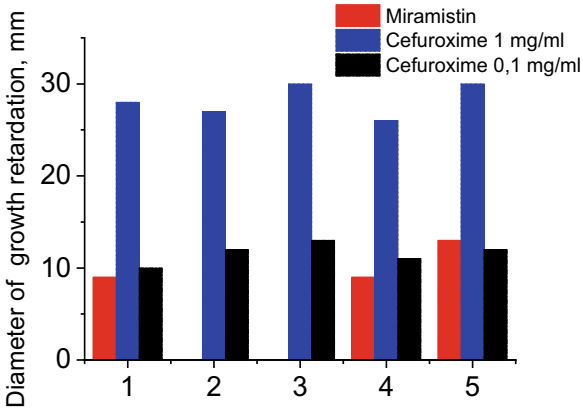

Fig. 21.20 Antimicrobial activity of hydrogels (1) PAA-0,4-Cef; (2) D20-PAA-0.4-Cef; (3) D100-PAA-0.4-Cef; (4) D500-PAA-0.4-Cef, and (5) DSS500-PAA-0.4-Cef against *S. aureus*

White outbred rats were used to evaluate the therapeutic properties of hydrogel coatings in vivo. The rat wounds were infected with *S. aureus*, *E. coli,* and *Klebsiella spp* (10^8 CFU/ml). The wound was then covered with hydrogels loaded with Cefuroxime (1 mg/ml) or miramistin (0.1 mg/ml) and standard tissue material (gauze bandage) for 24 h. Miramistin was used as an antibacterial agent for control experiments. After the bandage was removed, the wounds were tested for microorganisms. No gram-negative bacteria and very few gram-positive colonies were detected when Cefuroxime-coated hydrogel wounds were applied (Fig. 21.21c). Their efficacy was higher then miramistin-loaded hydrogels (Fig. 21.21b). In the case of classical gauze dressings, a significant number of colonies of bacteria of the studied strains were found (Fig. 21.21a).

Thus, hydrogels based on branched copolymers containing dextran as a structure-forming component can be used as containers for drugs, in particular antibiotics. When locally applied, they have demonstrated their effectiveness against a mixture of pathogenic bacteria, significantly inhibiting the growth of microorganisms on the infected wound surface. In vivo experiments confirm that antimicrobial hydrogels are promising biomaterials that provide rapid healing of superficial wounds.

Fig. 21.21 Rats wounds after removal of bandages after 24 h: **a** classic gauze bandage; **b** hydrogel D500-PAA-0.4, saturated with miramistin; and **c** hydrogel D500-PAA-0.4, saturated with Cefuroxime

21.5 Conclusion

Methods of synthesis and prospects of using hydrogels as biomedical materials are shown. Data on the synthesis and characterization of chemically cross-linked hydrogels based on branched copolymers of acrylamide with dextran as a structure-forming component are presented. The synthesis of ionic to nonionic hydrogels due to variation of dextan and its sulfodextran derivative and saponification of polyacrylamide units in the hydrogel are described.

The dependence of physicochemical properties of hydrogels on (a) chemical structure of polymers, (b) cross-linker concentration, and (c) internal structure of the network is shown. The efficiency of sorption properties of the obtained hydrogels for the creation of systems with drugs, silver nanoparticles, and biologically active substances has been proved.

The synthesis and characterization of nanocomposites with silver nanoparticles based on ionic and nonionic hydrogels are described, and the prospects of their use as antibacterial coatings for open wounds are shown. The advantages of the photochemical method of obtaining nanoparticles in hydrogels as nanocontainers are noted. It is proved that such nanosystems are stable and have a nanoparticle of suitable size for use in in vitro experiments.

In experiments with hydrogels saturated with biologically active dyes as photosensitizers, their antibacterial activity under irradiation with light of different wavelengths was shown. The research revealed hydrogel/dye materials effectiveness for antibacterial photodynamic therapy of open wounds of various genesis. Hydrogels based on branched copolymers containing dextran-polyacrylamide can be used as containers for drugs.

References

1. Hoffman AS (2002) Hydrogels for biomedical applications. Adv Drug Deliv Rev 43:3–12
2. Peppas NA, Bures P, Leobandung W, Ichikawa H (2000) Hydrogels in pharmaceutical formulations. Eur J Pharm Biopharm 50:27–46

3. Peppas NA, Huang Y, Torres-Lugo M, Ward JH, Zhang J (2000) Physicochemical foundations and structural design of hydrogels in medicine and biology. Annu Rev Biomed Eng 2:9–29
4. Ahmed EM (2015) Hydrogel: Preparation, characterization, and applications. J Adv Res 6:105–121
5. Hadjichristidis N, Pitsikalis M, Pispas S, Iatrou H (2001) Polymers with complex architecture by living anionic polymerization. Chem Rev 101(12):3747–3792
6. Gao H, Matyjaszewski K (2009) Synthesis of functional polymers with controlled architecture by CRP of monomers in the presence of cross-linkers: from stars to gels. Prog Polym Sci 34(4):317–350
7. Blencowe A, Tan JF, Goh TK, Qiao GG (2009) Core cross-linked star polymers via controlled radical polymerisation. Polymer 50(1):5–32
8. Kumar D, Khan N, Kumar P (2016) Improve the native characteristics of polysaccharides by grafting through the gamma radiation: a review. Green Chem and Tech Lett 2(3):151–159
9. Kumar D, Pandey J, Kumar P (2018) Microwave assisted synthesis of binary grafted psyllium and its utility in anticancer formulation. Carbohydr Polym 179:408–414
10. Xie W, Xu P, Wang W, Liu Q (2002) Preparation and antibacterial activity of a watersoluble chitosan derivative. Carbohydr Polym 50(1):35–40
11. Kaith B, Kumar K (2007) In air synthesis of Psy-cl-poly (AAm) network and its application in water-absorption from oil-water emulsions. Express Polym Lett 1(1):474–480
12. Kumar D, Kumar S (2014) Grafting of acrylic acid on to Plantago psyllium mucilage IOSR. J Appl Chem (IOSR-JAC) 7:76–82
13. Kumar D, Chandra R, Dubey R (2016) Synthesis and characterisation of cross-linked polymers of acrylic acid and psyllium mucilage (Psy-cl-AA). J Technol Adv Scient Res 2:185–189
14. Kumar D, Pandey J, Khan N, Kumar P, Kundu PP (2019) Synthesize and characterization of binary grafted psyllium for removing toxic mercury (II) ions from aqueous solution. Mater Sci Eng 104:109900
15. Kutsevol NV, Chumachenko VA, Rawiso M, Shkodich VF, Stoyanov OV (2015) Star-like dextran-polyacrylamide polymers: prospects of use in nanotechnologies J. Struct Chem 56(5):959–966
16. Kutsevol N, Guenet JM, Melnyk N, Sarazin D, Rochas C (2006) Solution properties of dextran-polyacrylamide graft copolymers. Polymer 47:2061–2068
17. Plieva F, Oknianska A, Degerman E, Galaev IY, Mattiasson B (2006) Novel supermacroporous dextran gels. J Biomat Sci 17(10):1075–1092
18. Nadtoka O, Kutsevol N, Krysa V, Krysa B (2018) Hybrid polyacryamide hydrogels: synthesis, properties and prospects of application. Mol Cryst Liq Cryst 672(1, 2):1–10
19. Nadtoka O, Virych P, Kutsevol N (2020) Hydrogels loaded with methylene blue: sorption-desorption and antimicrobial photoactivation study. Int J Polym Sci 2020:9875290
20. Ye Zh, Qin X, Lai N (2013) Synthesis and performance of an acrylamide copolymer containing nano-SiO_2 as enhanced oil recovery chemical. J Chem ID 437309. https://doi.org/10.1155/2013/437309
21. Nho YC, Park JS, Lim YM (2014) Preparation of poly(acrylic acid) hydrogel by radiation crosslinking and its application for mucoadhesives. Polymers 6:890–898
22. Nadtoka O, Virych P, Kutsevol N (2020) Investigation of swelling behavior of PAA and D-PAA hydrogels. Springer Proc Phys 247:47–60
23. Kutsevol NV, Chumachenko VA, Rawiso M, Shkodich VF, Stoyanov OV (2015) Star-like polymers dextran-polyacrylamide: the prospects *of* application for nanotechnology. J Struct Chem 56(5):1016–1023
24. Zhao Y, Su H, Fang L, Tan T (2005) Superabsorbent hydrogels from poly(asparticacid) with salt, temperature and pH-responsiveness properties. Polymer 46:5368–5376
25. Lagergren S (1898) About the theory of socalled adsorption of soluble substances. Kungl Svenska Vetenskapsakad Handl 24:1–39
26. Demirbas A (2004) Adsorption of lead and cadmium ions aqueous solutions onto modified lignin from alkali glycerol delignication. J Hazard Mater B 109:221–226

27. Nadtoka O, Kutsevol N, Naumenko AP, Virych PA (2019) Photochemical synthesis and characterization of hydrogel–silver nanoparticle composites. Res Chem Intermed. https://doi.org/10.1007/s11164-019-03891-4
28. Cooper R (2004) A review of the evidence for the use of topical antimicrobial agents in wound care World wide wounds 2004:1–11
29. Michielsen S, Churchward G, Bozia J, Stojilokivic I, Anic S (2006) Light activated antiviral materials and devices and methods for decontaminating virus infected environments. US 20070238660A1.
30. Nadtoka O, Virych P, Kutsevol N (2021) Synthesis and absorption properties of hybrid polyacrylamide hydrogels. Mol Cryst Liq Cryst 719(1):84–93
31. Kemnitz CR, Loewen MJ (2007) "Amide resonance" correlates with a breadth of c−n rotation barriers. J Am Chem Soc 129(9):2521–2528
32. Thoniyot P, Tan MJ, Karim AA, Young DJ, Loh XJ (2015) Nanoparticle-hydrogel composites: concept, design and applications of these promising, multi-functional materials. Adv Sci 2(1–2):1400010
33. Varaprasad K, Murali Mohan Y, Ravindra S, Narayana Reddy N, Vimala K, Monika K, Sreedhar B, Mohana Raju K (2010) Hydrogel-silver nanoparticle composites: a new generation of antimicrobials. J App Polymer Sci 115:1199–1207
34. Pradhan N, Jana NR, Mallick K, Pal T (2000) Seed mediated growth: a convenient way for size control in nanoparticle synthesis. J Surface Sci Technol 16:188–199
35. Winter GD (1962) Formation of the scab and the rate of epithelization of superficial wounds in the skin of the young domestic pig. Nature 193:293–294
36. Peppas NA, Bures P, Leobandung W, Ichikawa H (2000) Hydrogels in pharmaceutical formulations. Eur J Pharm Biopharm 50(1):27–46
37. Boehle KE (2017) Utilizing paper-based devices for antimicrobial resistant bacteria detection. Angew Chem 56(24):6886–6890
38. Li S, Dong S, Xu W, Tu S, Yan L, Zhao C, Chen X (2018) Antibacterial hydrogels. Adv Sci 5(5):1700527
39. Liao C, Li Y, Tjong SC (2019) Bactericidal and cytotoxic properties of silver nanoparticles. Int J Mol Sci 20(2):449
40. Nadtoka O, Virych P, Bezugla T, Yeshchenko O, Kutsevol N (2021) Antibacterial hybrid hydrogels loaded with nano silver. Appl. Nanosci. https://doi.org/10.1007/s13204-021-01706-w
41. Xiu ZM, Ma J, Balvarez PJJ (2011) Differential effect of common ligands and molecular oxygen on antimicrobial activity of silver nanoparticles versus silver ions. Environ Sci Technol 45:9003–9008
42. Knetsch MLW, Koole LH (2011) New strategies in the development of antimicrobial coatings: the example of increasing usage of silver and silver nanoparticles. Polymers 3(1):340–366
43. Suresh AK, Pelletier DA, Wang W, Morrell-Falvey JL, Gu B, Doktycz MJ (2012) Cytotoxicity induced by engineered silver nanocrystallites is dependent on surface coatings and cell types. Langmuir 28:2727–2735
44. Virych P, Nadtoka O, Virych P, Martynyuk V, Krysa V, Krysa B, Kutsevol N (2021) Photoinactivation *in vitro* of *Staphylococcus aureus* by visible light of different wavelengths. Interdisciplinary Stud Complex Syst 18:40–50
45. Nadtoka O, Kutsevol N, Linnik O, Nikiforov M (2019) Nanocomposite hydrogels containing silver nanoparticles as materials for wound dressings. Springer Proc Phys 222:375–387
46. Ramakrishnan P, Maclean M, MacGregor S, Anderson J, Grant M (2016) Cytotoxic responses to 405 nm light exposure in mammalian and bacterial cells: Involvement of reactive oxygen species Toxicol *In Vitro* 33:54–62
47. Ashkenazi H, Malik Z, Harth Y, Nitzan Y (2003) Eradication of Propionibacterium acnes by its endogenic porphyrins after illumination with high intensity blue light. FEMS Immunol Med Microbiol 35(1):17–24
48. Guffey J, Wilborn J (2006) *In vitro* bactericidal effects of 405-nm and 470-nm blue light. Photomed Laser Surg 24(6):684–688

49. Mahmoudi H, Bahador A, Pourhajibagher M, Alikhani M (2018) Antimicrobial photodynamic therapy: an effective alternative approach to control bacterial infections. J Lasers Med Sci 9(3):154–160
50. Li S, Dong S, Xu W (2018) Antibacter Hydrogels Adv Sci 5(5):1700527
51. Lehtopolku M, Kotilainen P, Puukka P (2012) Inaccuracy of the disk diffusion method compared with the agar dilution method for susceptibility testing of *Campylobacter spp.* J Clin Microbiol 50(1):52–56
52. Veiga S, Schneider JP (2013) Antimicrobial hydrogels for the treatment of infection. Biopolymers 100(6):637–644
53. Yang K, Han Q, Chen B (2018) Antimicrobial hydrogels: promising materials for medical application. Int J Nanomed 13:2217–2263
54. Tamahkar E, Özkahraman B, Süloğlu AK, İdil N, Perçin I (2020) A novel multilayer hydrogel wound dressing for antibiotic release. J Drug Deliv Sci Technol 58:101536